Approach to the thermodynamic limit in lattice QCD at $\mu \neq 0$

K. Splittorff[1] and J. J. M. Verbaarschot[1,2,3]

[1]*The Niels Bohr Institute, Blegdamsvej 17, DK-2100, Copenhagen Ø, Denmark*
[2]*Niels Bohr International Academy, Blegdamsvej 17, DK-2100, Copenhagen Ø, Denmark*
[3]*Department of Physics and Astronomy, SUNY, Stony Brook, New York 11794, USA*

The expectation value of the complex phase factor of the fermion determinant is computed to leading order in the p expansion of the chiral Lagrangian. The computation is valid for $\mu < m_\pi/2$ and determines the dependence of the sign problem on the volume and on the geometric shape of the volume. In the thermodynamic limit with $L_i \to \infty$ at fixed temperature $1/L_0$, the average phase factor vanishes. In the low temperature limit where L_i/L_0 is fixed as L_i becomes large, the average phase factor approaches 1 for $\mu < m_\pi/2$. The results for a finite volume compare well with lattice results obtained by Allton *et al.* After taking appropriate limits, we reproduce previously derived results for the ϵ regime and for one-dimensional QCD. The distribution of the phase itself is also computed.

PACS numbers: 12.38.Gc, 11.30.Rd

I. INTRODUCTION

Numerical lattice QCD at nonzero baryon chemical potential is obstructed by the sign problem: At nonzero chemical potential, μ, the phase factor of the fermion determinant

$$e^{2i\theta} = \frac{\det(D + \mu\gamma_0 + m)}{\det(D + \mu\gamma_0 + m)^*} \qquad (1)$$

invalidates a direct application of Monte Carlo methods. However, indirect methods have been devised to circumvent the sign problem [1–16]. Since these approaches only apply when the average of the phase factor is close to unity, it is of considerable interest to understand when the fluctuations of the phase are mild and when they are severe. Since the measurement of the average phase factor on the lattice is plagued by the sign problem as well, it is imperative to understand the average phase factor analytically.

In this paper we study the average phase factor analytically within chiral perturbation theory. In particular, the approach to the thermodynamic limit will be analyzed.

Despite the absence of baryons, chiral perturbation theory has proved a vital tool in understanding lattice simulations at nonzero baryon chemical potential. The generating functional for the eigenvalue density of the QCD Dirac operator includes quarks with the opposite sign of the chemical potential [17], which therefore couple to the third component of isospin. Using this fact, the exact quenched [18] and unquenched [19,20] microscopic spectral densities of the QCD Dirac operator were derived from a chiral Lagrangian. This result revealed that, at nonzero chemical potential, the chiral condensate is related to the spectral density by a mechanism that is different from the Banks Casher relation [21]: The discontinuity in the chiral condensate is due to complex oscillations on the microscopic scale [22] in a macroscopic region of the complex eigenvalue plane.

The microscopic limit is also known as the ϵ domain of QCD. Microscopic results for QCD can equally well be derived by means of chiral random matrix theory [23,24]. This has the advantage that one may employ powerful random matrix methods such as orthogonal polynomials [25–28], the replica trick [29], or the supersymmetric method [30]. For example, the unquenched microscopic spectral density at nonzero chemical potential was first derived by means of random matrix theory [19], whereas the quenched spectral density at nonzero chemical potential was first obtained by means of the replica trick in combination with the Toda lattice equation [18].

The recent computation of the average phase factor in the microscopic domain [31,32] shows that the average phase factor is suppressed exponentially with the volume when $\mu > m_\pi/2$. For such values of the chemical potential, the quark mass is inside the cloud of eigenvalues of the Dirac operator, and numerical lattice QCD simulations become exceedingly difficult. For smaller values of the chemical potential, the quark mass is outside the two-dimensional domain of the eigenvalues, and the sign problem is less severe.

In this paper we examine the character of the sign problem in the region $\mu < m_\pi/2$ and temperatures such that the use of chiral perturbation theory can be justified. With $\mu < m_\pi/2$ it was found in [31,32] that the average phase factor remains nonzero in the microscopic limit where $\mu F_\pi \sqrt{V}$ is held fixed as the volume is taken to infinity. For $\mu F_\pi \sqrt{V} \gg 1$ the large volume asymptotic limit of the microscopic prediction is simply given by

$$\langle e^{2i\theta}\rangle_{N_f} = \left(1 - \frac{4\mu^2}{m_\pi^2}\right)^{N_f+1}, \qquad \mu < m_\pi/2. \qquad (2)$$

(The quenched and the phase-quenched average of the phase factor give identical predictions in this limit. Both are obtained by setting $N_f = 0$ in the equation above.) This

result suggests that unquenched lattice simulations in this domain are feasible.

Here we examine whether the average phase factor remains nonzero for $\mu < m_\pi/2$ when we relax the microscopic constraints and approach the thermodynamic limit at fixed chemical potential. In order to do so, we compute the average phase factor using the p expansion of chiral perturbation theory where

$$p \sim 1/L, \qquad m_\pi \sim 1/L, \qquad \mu \sim 1/L, \qquad T \sim 1/L, \tag{3}$$

and work to leading (one-loop) order. The previous calculation of the average phase factor was worked out [31,32] in the microscopic domain where $m_\pi^2 F_\pi^2 \sim 1/V$ and $\mu^2 F_\pi^2 \sim 1/V$ as the volume is taken to infinity. The new one-loop computation presented here includes the effect generated by the nonzero momentum modes of the Goldstone bosons. We keep explicitly the dependence on volume $V = L_i^3 L_0$ and the ratios L_0/L_i in order to study the approach to the thermodynamic limit. The new result bridges the gap between the microscopic prediction [31,32] and the parameter range typically used in lattice gauge theories. This allows us to compare the one-loop result for the average phase factor to lattice results by Allton *et al.* Below the pseudocritical temperature for chiral symmetry restoration, the lattice results are in remarkably good agreement with the analytical predictions.

The distribution of the phase itself (rather than the phase factor) also follows from the one-loop computation. We give the explicit form of the distribution of the phase to one-loop order in chiral perturbation theory.

The paper is organized as follows. In the next section we present the general setup for computing the one-loop result for the average phase factor within chiral perturbation theory. The explicit one-loop result is derived in Sec. III. This expression is evaluated numerically in Sec. IV, and the comparison to lattice data is made in Sec. V. The effect of a finite box on the average phase factor is further discussed in Sec. VI. Section VII contains the discussion of the distribution of the phase. We end with concluding remarks in Sec. VIII.

II. THE AVERAGE PHASE FACTOR TO LEADING ORDER

Gauge field configurations can only be generated by Monte Carlo simulations if the integration measure is non-negative. If the fermion determinant has a nontrivial phase, the sign problem can, in principle, be solved by reweighting [1,5,6], where the expectation value of an operator is calculated according to

$$\frac{\langle \mathcal{O}\det^{N_f}(D + \mu\gamma_0 + m)\rangle}{\langle \det^{N_f}(D + \mu\gamma_0 + m)\rangle} = \frac{\langle \mathcal{O}e^{iN_f\theta}|\det^{N_f}(D + \mu\gamma_0 + m)|\rangle}{\langle|\det^{N_f}(D + \mu\gamma_0 + m)|\rangle} \left[\frac{\langle e^{iN_f\theta}|\det^{N_f}(D + \mu\gamma_0 + m)|\rangle}{\langle|\det^{N_f}(D + \mu\gamma_0 + m)|\rangle}\right]^{-1}. \tag{4}$$

Obviously, the success of this method is determined by the expectation value of the phase factor, which is our main motivation to study the average phase factor. Reweighting is not unique and one could, for example, average with respect to the theory at zero chemical potential. For that reason we will study different averages of the phase factor, the average with respect to the full QCD partition function and the average with respect to the phase-quenched partition function, as well as an average with dynamical quarks at zero chemical potential.

Like reweighting, the complex Langevin method [2–4] and the density of states method [14–16] are expected to fail for a strongly fluctuating phase factor. Methods that rely on analytical continuation [7–13] could, in principle, work even for a strongly fluctuating phase factor. Note, however, that the average phase factor is nonanalytic at zero chemical potential [32].

The average phase factor in the full theory is the ratio of two partition functions: a partition function with an extra fermionic quark as well as a conjugate bosonic quark divided by the usual QCD partition function

$$\langle e^{2i\theta}\rangle_{N_f} = \frac{\langle \det^{N_f+1}(D + \mu\gamma_0 + m)/\det(D - \mu\gamma_0 + m)\rangle}{\langle \det(D + \mu\gamma_0 + m)^{N_f}\rangle}. \tag{5}$$

Here we used that conjugate quarks correspond to ordinary quarks with the opposite sign of the chemical potential [33]. With the usual setup of leading order chiral perturbation theory (see for example [34,35]), the free energy is a sum of contributions from each of the Goldstone bosons. The contributions to the numerator of pions with no isospin charge cancel against contributions from the denominator. This leaves us with

$$\langle e^{2i\theta}\rangle_{N_f} = e^{(N_f+1)(G_0(\mu=0)-G_0(\mu))}, \tag{6}$$

where each G_0 includes the contribution of two oppositely charged Goldstone modes. In order to get the combinatorics right, notice that the inverse determinant in (5) represents a conjugate bosonic quark. The charged Goldstone bosons contain this bosonic quark in addition to one of the $N_f + 1$ fermionic quarks and are thus fermionic in nature, resulting in an additional minus sign from the fermionic loop.

Because of the sign problem, one often studies averages in the phase-quenched theory where the phase of the fermion is ignored,

$$Z_{1+1^*} = \langle|\det(D + \mu\gamma_0 + m)|^2\rangle. \tag{7}$$

The average phase factor in the phase-quenched theory is

defined by

$$\langle e^{2i\theta}\rangle_{1+1^*} = \frac{\langle \det^2(D + \mu\gamma_0 + m)\rangle}{\langle |\det(D + \mu\gamma_0 + m)|^2\rangle} = \frac{Z_{N_f=2}}{Z_{1+1^*}}. \qquad (8)$$

To leading order in chiral perturbation theory this ratio is given by

$$\langle e^{2i\theta}\rangle_{1+1^*} = e^{G_0(\mu=0)-G_0(\mu)}. \qquad (9)$$

Notice that this result coincides with the one-loop result for the quenched theory (with no dynamical quarks) obtained from (6) by setting $N_f = 0$, as well as with the result for partially quenched computations with dynamical quarks at zero chemical potential.

   In summary, to determine the average phase factor to one-loop order, all that is required is the difference between $G_0(\mu)$ and $G_0(\mu = 0)$. We will derive this difference in Sec. III.

III. EVALUATION OF $G_0(\mu) - G_0(\mu = 0)$

   As we are particularly interested in the approach to the thermodynamic limit, we will consider a finite system with volume $V = L_i^3 L_0$. Hasenfratz and Leutwyler [34] worked out G_0 for $\mu = 0$. This calculation was generalized to nonzero chemical potential in [32]. For completeness, we repeat the main steps of the computation below.

   Consider a single charged Goldstone boson with charge 2 in a box $V = L_i^3 L_0$. The one-loop contribution to the partition function is given by

$$e^{G_0(\mu)/2} \equiv \exp\left[-\frac{1}{2}\sum_{p_{k\alpha}} \log(\vec{p}_k^2 + m_\pi^2 + (p_{k0} - 2i\mu)^2) \right], \qquad (10)$$

where

$$p_{k\alpha} = \frac{2\pi k_\alpha}{L_\alpha}, \qquad k_\alpha \text{ integer.} \qquad (11)$$

While $G_0(\mu)$ is divergent, the difference between $G_0(\mu)$ and $G_0(\mu)$ for $V = \infty$ is finite, that is,

$$G_0(\mu) = G_0(\mu)|_{V=\infty} + g_0(\mu) \qquad (12)$$

with $g_0(\mu)$ finite. The p_0-integration contour in the second term of the difference

$$\begin{aligned}
&G_0(\mu)|_{V\to\infty} - G_0(\mu = 0)|_{V\to\infty} \\
&= \int p^{d-1}dp\,dp_0[\log(\vec{p}^2 + m_\pi^2 + p_0^2) \\
&\quad - \log(\vec{p}^2 + m_\pi^2 + (p_0 - 2i\mu)^2)]
\end{aligned}$$

can be shifted by $2i\mu$ if there are no obstructions from singularities. This is the case if $2\mu < m_\pi$, so that the μ dependence resides entirely in $g_0(\mu)$. The difference of the free energies in (6) and (9) is thus given by the difference of the finite parts,

$$G_0(\mu) - G_0(\mu = 0) = g_0(\mu) - g_0(\mu = 0). \qquad (13)$$

This also shows that the average phase factor does not depend on the ultraviolet cutoff. The infrared nature of the average phase factor has been verified on the lattice [36].

   After several manipulations, including Poisson resummation and Jacobi's imaginary transformation (the steps are given in detail in [32]), we find two equivalent representations of $g_0(\mu)$, both valid for $\mu < m_\pi/2$,

$$\begin{aligned}
g_0(\mu) = &\int_0^\infty \frac{d\lambda}{\lambda^3} e^{-m_\pi^2 L^2 \lambda/4\pi} \\
&\times \left(\prod_{\alpha=0}^3 \sum_{l_\alpha} e^{-2\mu l_0 L_0 \delta_{\alpha 0}} e^{-\pi(l_\alpha^2 L_\alpha^2/\lambda L^2)} - 1 \right) \qquad (14)
\end{aligned}$$

and

$$\begin{aligned}
g_0(\mu) = &\int_0^1 \frac{d\lambda}{\lambda^3} e^{-m_\pi^2 L^2 \lambda/4\pi} \left(\prod_{\alpha=0}^3 \sum_{l_\alpha} e^{-2\mu l_0 L_0 \delta_{\alpha 0}} e^{-\pi(l_\alpha^2 L_\alpha^2/\lambda L^2)} - 1 \right) \\
&+ \int_0^1 \frac{d\lambda}{\lambda} e^{\mu^2 L^2/\pi\lambda} e^{-m_\pi^2 L^2/(4\pi\lambda)} \left(\prod_{\alpha=0}^3 \sum_{l_\alpha} e^{-2i\mu l_0 (L^2/L_0\lambda)\delta_{\alpha 0}} e^{-\pi l_\alpha^2 (L^2/L_\alpha^2 \lambda)} - 1 \right) + \int_1^\infty \frac{d\lambda}{\lambda} e^{\mu^2 L^2 \lambda/\pi} e^{-m_\pi^2 L^2 \lambda/4\pi} \\
&- \int_1^\infty \frac{d\lambda}{\lambda^3} e^{-m_\pi^2 L^2 \lambda/4\pi}, \qquad (15)
\end{aligned}$$

where l_α runs over all integers and we have introduced the length

$$L \equiv (L_0 L_i^3)^{1/4}. \qquad (16)$$

The first representation has the advantage that the chemical potential explicitly appears in the combination μL_0. (Note that L_0 also appears in other places.) The second represen-

tation can be used to expand the result in a power series in m_π^2 and μ^2. It also may be preferable for numerical evaluations.

   The one-loop result is valid for $L\Lambda_{\text{QCD}} \gg 1$, $mV\Sigma \gg 1$ and both $m_\pi \ll \Lambda_{\text{QCD}}$ and $\mu \ll \Lambda_{\text{QCD}}$. Finally, the condition $\mu < m_\pi/2$ has to be satisfied. The reason is that, for $\mu > m_\pi/2$, the Goldstone fields have to be expanded about

a rotated ground state. For $m_\pi^2 L^2 \ll 1$ and $\mu^2 L^2 \ll 1$ the dominant contribution is given by the zero-momentum term and the one-loop result reduces to (2). A small $m_\pi L$ and small μL expansion about this result was given in [32]. The general one-loop result is also valid when $m_\pi^2 L^2$ and $\mu^2 L^2$ are of order or larger than 1. In the next section we study the one-loop result numerically.

IV. NUMERICAL EVALUATION OF THE ONE-LOOP RESULT

In this section we study the one-loop expression for the average phase factor as a function of dimensionless combinations of the parameters. The average phase factor depends only on three dimensionless combinations:

$$m_\pi L, \quad \mu L, \quad \text{and} \quad \frac{L_0}{L_i}. \tag{17}$$

As the one-loop expression is only valid for $\mu < m_\pi/2$, we will express our results as a function of the ratio $\mu/(m_\pi/2)$. We will consider 3 different cases: (1) *the thermodynamic limit at fixed temperature* where $L_i m_\pi$ becomes large while $L_0 m_\pi$ remains fixed, (2) *the thermodynamic limit at low temperatures* where $L_i m_\pi$ grows for fixed asymmetry L_i/L_0, and (3) *the low temperature limit in a finite box* where $L_0 m_\pi$ increases for fixed $L_i m_\pi$.

Thermodynamic limit at fixed temperature.—The thermodynamic limit at fixed temperature is obtained by letting the spatial extent of the box in units of the inverse pion mass go to infinity while keeping the temporal extent also in units of $1/m_\pi$ fixed. In this limit the sign problem is acute for any nonzero value of the baryon chemical potential, as indicated by a vanishing average phase factor. In Fig. 1 we show the approach of the average phase factor to zero as L_i increases. The two left plots show the phase-quenched prediction (which, as discussed above, is equivalent to the quenched prediction), while the two right plots show the case with two dynamical flavors. Note that for $L_i < L_0$ the average phase factor is dominated by the static pion modes, cf. (2) [55].

Thermodynamic limit with temperature going to zero.— As is common practice in lattice QCD, we now fix the asymmetry of the box, L_i/L_0, and vary the size of the box. A large box now automatically implies a low temperature. In this thermodynamic limit the average phase factor approaches unity as long as the chemical potential is less than half of the pion mass. For larger values of the chemical potential the average phase factor is zero. In Fig. 2 we show the approach to this step function as a function of L_i. The
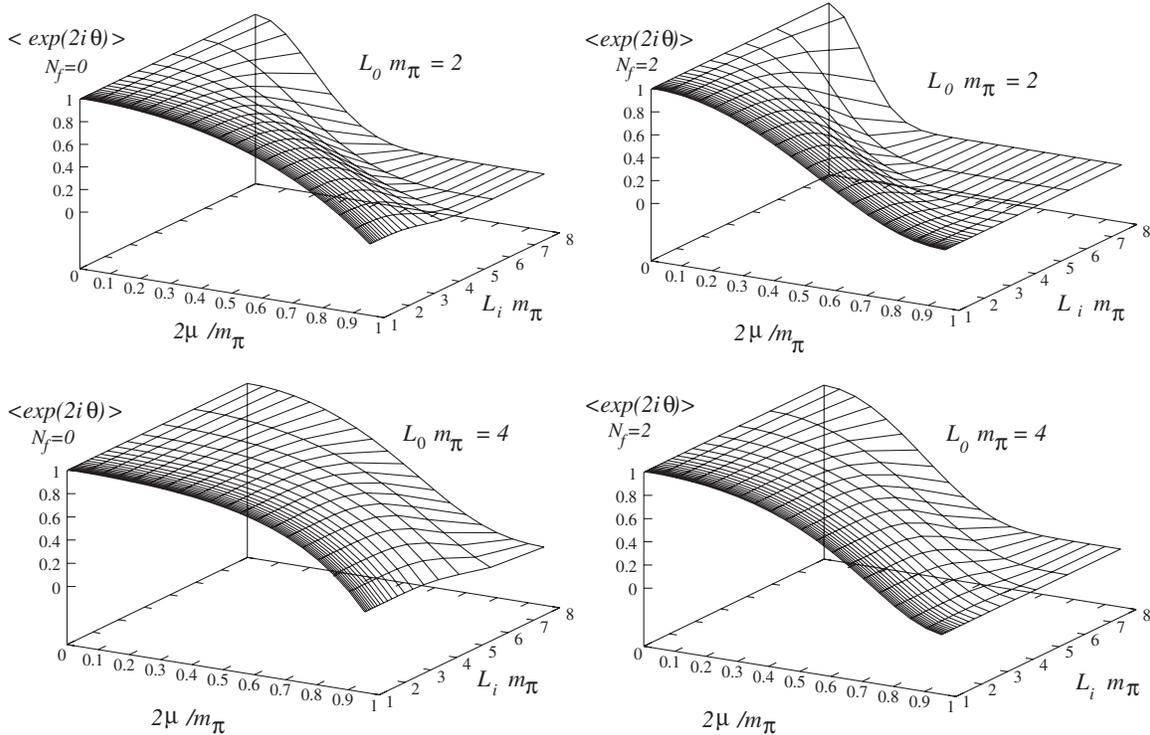

FIG. 1. The average phase factor goes to zero as the spatial extent of the box (in units of $1/m_\pi$) becomes large as compared to the temporal extent. The approach to the thermodynamic limit is illustrated by varying $m_\pi L_i$ at fixed temperature $1/L_0$. Left panels: The (phase) quenched average phase factor. Right panels: The average phase factor with two dynamical flavors with the same mass. Top panels: $m_\pi L_0 = 2$. Bottom panels: $m_\pi L_0 = 4$. Note that the average phase factor starts dropping to zero when L_i exceeds L_0; the spatial length L_i needs to be larger than L_0 for the effect of the pion loop to be present in the average phase factor.
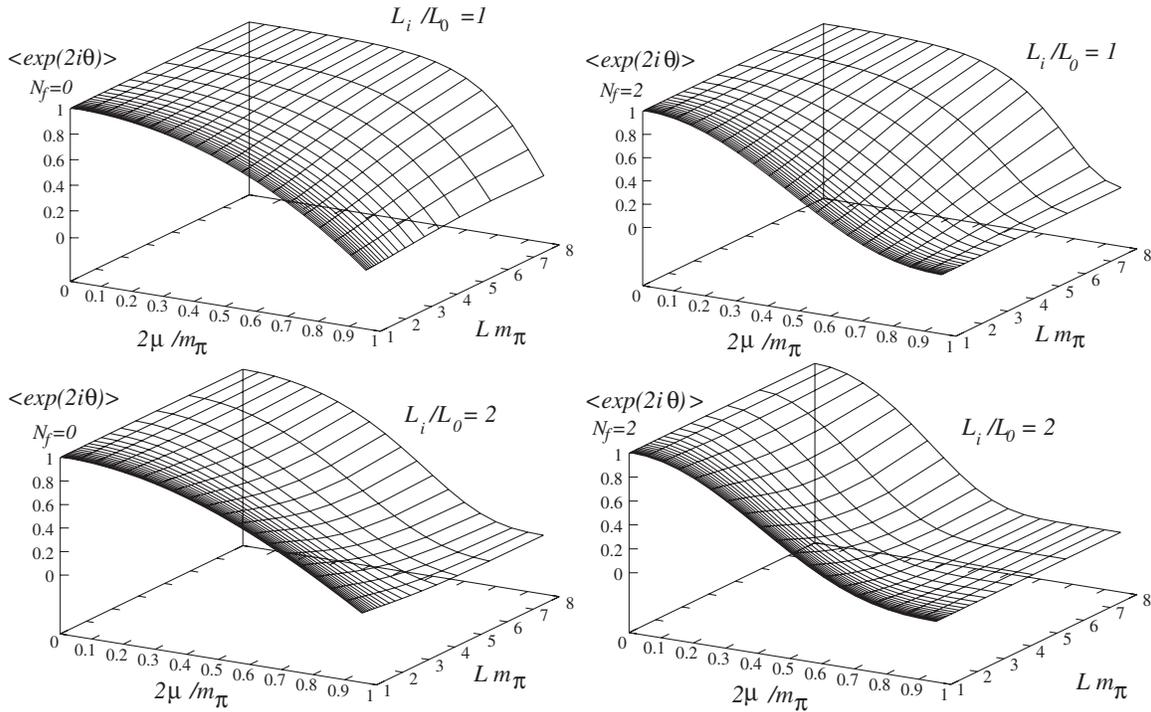
FIG. 2. The average phase factor when approaching the thermodynamic limit for fixed L_i/L_0. Left panels: The (phase) quenched case. Right panels: Two dynamical flavors. Top panels: The temporal extent of the box is taken equal to its spatial extent; hence, the y axis is also the inverse temperature in units of $1/m_\pi$. Bottom panels: The asymmetry is now set to $L_i/L_0 = 2$. Hence, the Lm_π is also $\sqrt{8}L_0 m_\pi$. In all cases, in the thermodynamic limit the average phase factor approaches a step function which becomes zero beyond $2\mu = m_\pi$.

two top panels are for a cubic box (quenched and un-quenched), and the two lower plots are for $L_i = 2L_0$. The approach to the step function is slower when the asymmetry is larger than unity.

Zero temperature in a finite box.—Here we consider the limit where the spatial size of the box is fixed in units of $1/m_\pi$ as the temperature (in units of m_π) is lowered. In the zero temperature limit where the asymmetry $L_i/L_0 \ll 1$, the average phase factor again approaches the step function $\theta(m_\pi - 2\mu)$. This is not surprising given that this behavior

was also found in the exact solution of one-dimensional QCD [37].

In Fig. 3 we show how the average phase factor, quenched (left panel) and unquenched (right panel), behaves as a function of μ and T in a finite box.

V. COMPARISON TO LATTICE DATA BY ALLTON *ET AL.*

The main limitations of lattice studies of QCD at non-zero chemical potential are the phase fluctuations of the
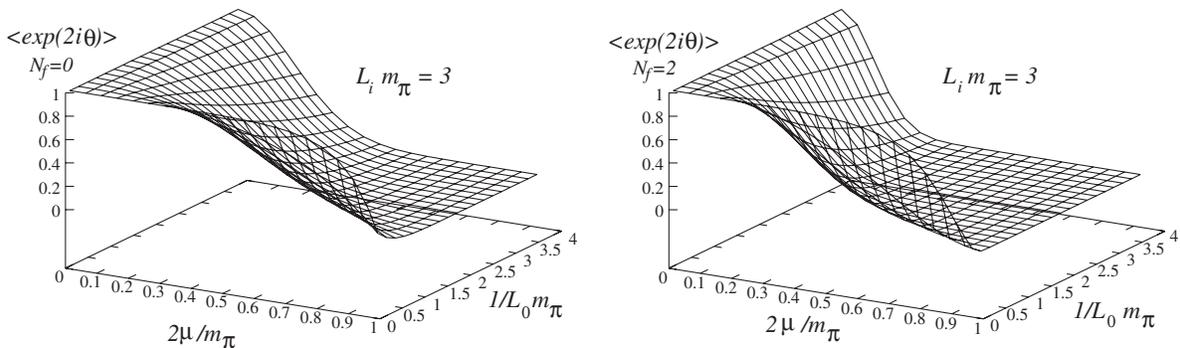

FIG. 3. The average phase factor for $m_\pi L_i = 3$. It approaches zero with increasing temperature. Left panel: The (phase) quenched case. Right panel: The $N_f = 2$ case. Notice that the zero temperature limit is the step function $\theta(m_\pi - 2\mu)$. In this limit the time direction is much longer than the spatial ones, and as expected, the step function found is consistent with the result from one-dimensional QCD [37].

fermion determinant, and it is natural to analyze them quantitatively [11,16,38–47]. In this section we compare the one-loop results obtained above to the lattice data of Allton *et al.* [13].

In [13] the response of the QCD partition function to a baryon and isospin chemical potential was measured at zero value of the chemical potential. The response to second order in the baryon and isospin chemical potential was given in terms of two numbers, c_2 and c_2^I, respectively (see Table 3.2 of [13]). They are related to the quark and isospin susceptibility at $\mu = 0$ according to

$$c_2 = \frac{\chi_q}{2T^2}, \qquad c_2^I = \frac{\chi_I}{2T^2}. \tag{18}$$

To second order in the chemical potential, the measured average phase factor (in the phase-quenched theory) is given by

$$\begin{aligned} \langle e^{2i\theta} \rangle_{\text{lat}} &= e^{L_i^3 T \mu^2 (c_2 - c_2^I)} \\ &= e^{(c_2 - c_2^I)(L_i/L_0)^3 (2\mu/m_\pi)^2 (m_\pi/T_c)^2/(T/T_c)^2/4}, \end{aligned} \tag{19}$$

where, in the second line, we have expressed the result in terms of accessible dimensionless ratios. Note that the strength of the sign problem to lowest order in the Taylor

expansion only depends on the coefficient of the off-diagonal susceptibility $c_2^{ud} \equiv (c_2 - c_2^I)/4$.

The one-loop chiral perturbation theory result is obtained by matching the dimensions of the box and the chemical potential in units of the inverse pion mass to those of [13]. To fix the scale we use the value $m_\pi/T_c = 3.58$ from [48]. For temperatures below the critical temperature, T_c, the agreement is very good; see Fig. 4. Since chiral perturbation theory is not applicable in the chirally restored phase, the disagreement for $T > T_c$ is as expected. Unfortunately, the isospin susceptibility was not calculated beyond second order in μ_I in [13], so we cannot extract the average phase factor to higher order. The fourth order term is of particular interest because the analytical one-loop result, displayed in Fig. 4, is well approximated by $\exp(-a\mu^2 - b\mu^4)$ where a and b are positive constants.

Beyond the critical temperature the severity of the sign problem decreases significantly. In the high temperature limit the difference from one of the average phase factor comes from terms of order g^4 and higher as can be inferred from [49,50]. Indeed, the terms up to order g^3 are functions of $\sum_f \mu_f^2$ so that the phase-quenched and the unquenched partition functions are identical up to this order. In lattice simulations by Allton *et al.* the quark and isospin suscep-
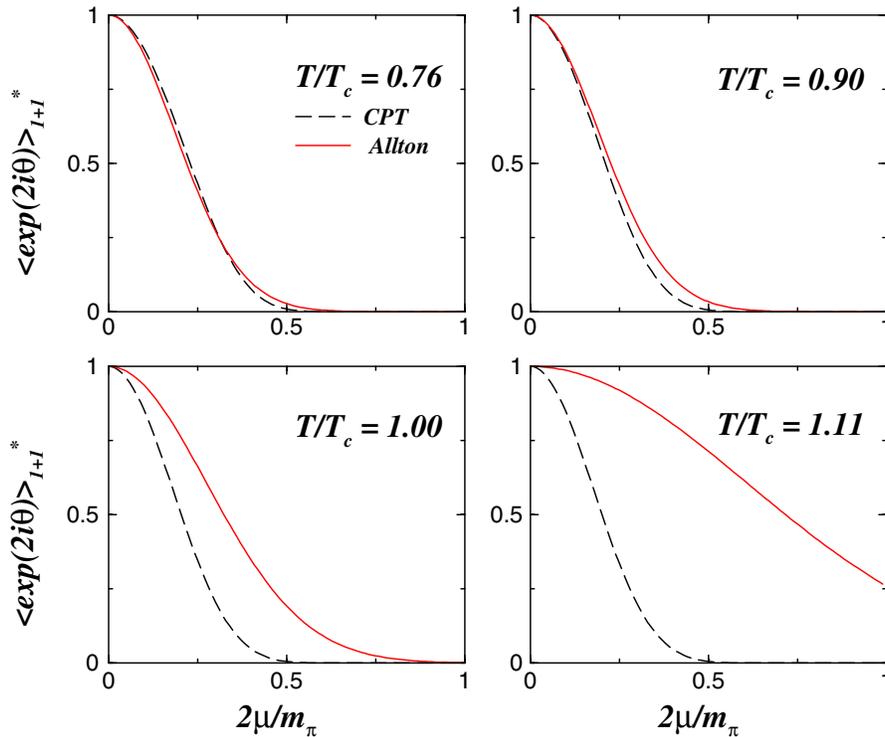

FIG. 4 (color online). The phase-quenched average phase factor obtained using the data of [13] (solid curves) compared with the result from chiral perturbation theory (dashed curves). The temperatures are $T/T_c = 0.76, 0.90, 1.00, 1.11$, where T_c is the critical temperature at $\mu = 0$. The agreement is good even close to T_c. Above the critical temperature the response to the baryon and isospin chemical potential becomes alike as bound states of quarks have melted. The prediction of chiral perturbation theory of course fails in this region.

tibilities are very close for $T > T_c$. The physical implication is that bound states of light quarks are absent beyond T_c.

VI. FINITE VERSUS INFINITE BOX

In this section we compare the result (15) for a finite box with its thermodynamic limit which has been used in the resonance gas model.

In the resonance gas model it is usually assumed that $L_i m_\pi \gg 1$ such that the spatial momenta in the expression for g_0 can be integrated over instead of a discrete summation. This leads to the standard expression

$$g_0(\mu) = \frac{V m_\pi^2 T^2}{\pi^2} \sum_{n=1}^{\infty} \frac{K_2(\frac{m_\pi n}{T})}{n^2} \cosh\left(\frac{2\mu n}{T}\right). \quad (20)$$

In addition, the resonance gas model includes heavier resonances. Among others, it was applied [51] to the quark and isospin susceptibilities for temperatures beyond T_c.

In Fig. 5 we compare the average phase factor in a box with finite spatial length to the result obtained using (20). We observe that the validity of the standard expression (20) depends on the chemical potential. This is not surprising. After all, the mass of the charged Goldstone modes is $m_\pi \pm 2\mu$ (recall that these Goldstone modes are made out of a quark and a conjugate quark). As μ approaches $m_\pi/2$ the lightest mode becomes massless, which invalidates the replacement the sum over momenta by an integral.

VII. THE DISTRIBUTION OF THE PHASE

In addition to studying the average phase factor, it is natural to also analyze the distribution function of the phase [39,52] itself. It is defined by
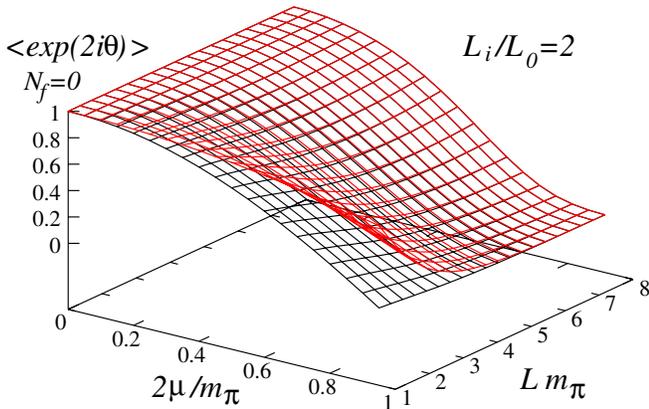

FIG. 5 (color online).   The average phase factor for a finite box (lower surface) compared to the result in the thermodynamic limit at fixed L_i/L_0 (upper surface). Notice that finite size corrections become more important as μ increases.

$$\rho_{N_f}(\theta) \equiv \langle \delta(\theta - \theta') \rangle_{N_f}$$

$$= \frac{\int dA |\det(D + \mu\gamma_0 + m)|^{N_f} e^{iN_f \theta'} \delta(\theta - \theta') e^{-S_{\text{YM}}}}{\int dA |\det(D + \mu\gamma_0 + m)|^{N_f} e^{iN_f \theta'} e^{-S_{\text{YM}}}}.$$

$$(21)$$

The unquenched θ distribution can be written

$$\rho_{N_f}(\theta) = e^{iN_f \theta} \rho_{N_f/2 + N_f/2^*}(\theta) \frac{Z_{N_f/2 + N_f/2^*}}{Z_{N_f}}, \quad (22)$$

where the phase-quenched θ distribution is defined as the average

$$\rho_{N_f/2 + N_f/2^*}(\theta) \equiv \langle \delta(\theta - \theta') \rangle_{N_f/2 + N_f/2^*} \quad (23)$$

with respect to the phase-quenched partition function

$$Z_{N_f/2 + N_f/2^*} = \langle |\det(D + \mu\gamma_0 + m)|^{N_f} \rangle. \quad (24)$$

This rewriting shows that the unquenched θ distribution is complex for any nonzero value of the chemical potential. The complex nature of the unquenched θ distribution resides entirely in $\exp(iN_f\theta)$—the other factors in (22) are real, positive, and even. Despite its simple form, the effect of the phase is drastic. Integrating over θ we find that

$$\int d\theta e^{iN_f\theta} \rho_{N_f/2 + N_f/2^*}(\theta) = \frac{Z_{N_f}}{Z_{N_f/2 + N_f/2^*}}, \quad (25)$$

which becomes exponentially small [$\sim \exp(-V)$] in the thermodynamic limit at fixed temperature.

In principle, one can extract the unquenched partition function from the phase-quenched one and the phase-quenched θ distribution using (25). Numerically, it is, however, very difficult to handle the detailed cancellations. It only works if the width of the θ distribution is comparable to $2\pi/N_f$ so that the complex oscillations have little effect. Below we will compute the θ distribution in a finite box using chiral perturbation theory and show that the width of the θ distribution is rather of order $\sqrt{V}$.

θ distribution to one loop in chiral perturbation theory

The distribution function of the phase, $\rho_{N_f}(\theta)$, can be extracted from the moments of the phase factor. Just like the average phase factor the higher moments follow from the one-loop computation

$$\langle e^{2ni\theta} \rangle_{N_f} = e^{n(N_f + n)(G_0(\mu=0) - G_0(\mu))}. \quad (26)$$

This holds for both positive and negative integers n. Using the replica trick [29,53], one can analytically continue n to noninteger values. For instance,

$$\langle e^{i\theta} \rangle_{N_f} = e^{1/2(N_f + 1/2)(G_0(\mu=0) - G_0(\mu))}. \quad (27)$$

We expect that the analytic continuation of $\langle \exp(2in\theta) \rangle$ in n is valid when the quark mass is outside the support of the eigenvalues—as is always the case in this paper.

In (26) we evaluated the even Fourier components. If we assume that the odd Fourier coefficients are given by the same expression, we can simply express the delta function in the definition of $\rho_{N_f}(\theta)$ into a sum over the moments. Introducing the shorthand

$$\Delta G_0 \equiv G_0(\mu) - G_0(\mu = 0) \tag{28}$$

we find

$$
\begin{aligned}
\rho_{N_f}(\theta) &= \frac{1}{\pi} \sum_{n=-\infty}^{\infty} e^{-in\theta - (n/2)((n/2)+N_f)\Delta G_0} \\
&= \frac{1}{\pi} e^{iN_f\theta + (1/4)N_f^2 \Delta G_0} \sum_{n=-\infty}^{\infty} e^{-in\theta - n^2 \Delta G_0/4} \\
&= \frac{1}{\pi} e^{iN_f\theta + (1/4)N_f^2 \Delta G_0} \vartheta_3(\theta/(2\pi), e^{-\Delta G_0/4}). \tag{29}
\end{aligned}
$$

By a Poisson resummation this can be rewritten as

$$\rho_{N_f}(\theta) = \frac{1}{\sqrt{\pi \Delta G_0}} e^{iN_f\theta + (1/4)N_f^2 \Delta G_0} \sum_n e^{-(\theta+2n\pi)^2/\Delta G_0}, \tag{30}$$

valid for a compact phase angle $\theta \in [-\pi, \pi]$. For a continuous phase angle, $\theta \in [-\infty, \infty]$, the distribution function becomes a simple Gaussian:

$$\rho_{N_f}(\theta) = \frac{1}{\sqrt{\Delta G_0 \pi}} e^{(N_f/2)^2 \Delta G_0} e^{iN_f\theta - \theta^2/\Delta G_0}. \tag{31}$$

The quenched as well as the phase-quenched averages are given by $\rho_{N_f=0}(\theta)$. Notice that result (31) is consistent with the general form given in (22). Since ΔG_0 is extensive, the width of the θ distribution is of order $\sqrt{V}$, while its amplitude increases exponentially with the volume. Along with the fact that the distribution is normalized to 1, this illustrates just how intricate the cancellations will be, and therefore how tough the sign problem will be to handle numerically.

With $\rho_{N_f}(\theta)$ at hand it is straightforward to also compute the variance of the phase

$$\langle \theta^2 \rangle_{N_f} - \langle \theta \rangle_{N_f}^2 = \tfrac{1}{2}\Delta G_0. \tag{32}$$

Note that the result is independent of N_f even though $\langle \theta^2 \rangle_{N_f}$ and $\langle \theta \rangle_{N_f}$ both depend on the number of flavors. This suggests that the variance of the phase can be obtained from the quenched theory.

The Gaussian form of the phase-quenched θ distribution is in agreement with the numerical result of Ejiri [52]. Notice, however, that an error of order $1/\sqrt{V}$ in the numerical determination of the width of the Gaussian will lead to an error of order 1 in the unquenched partition function; cf. (25). Small non-Gaussian corrections can have a similar dramatic effect. We expect that higher order terms in chiral perturbation theory as well as effects from baryons will result in a non-Gaussian form.

VIII. CONCLUSIONS

The average phase factor of the fermion determinant has been computed and examined to one-loop order in chiral perturbation theory for a quark chemical potential less than half of the pion mass. In the ordinary thermodynamic limit at fixed temperature, the average phase factor is zero for any nonzero value of the chemical potential. If the temperature is taken to zero at fixed aspect ratio of the box, the phase factor remains unity when the chemical potential is less than $m_\pi/2$. This indicates that QCD at zero temperature has a mild sign problem for $\mu < m_\pi/2$ in the thermodynamic limit. It would be of interest to study this region on the lattice—in particular, to examine if there is a spinodal line in this region.

The one-loop prediction for the average phase factor is in agreement with lattice data below the critical temperature. Below T_c the one-loop prediction thus gives a direct way to estimate the strength of the sign problem for a given lattice volume $V = L_i^3 L_0$ and quark mass.

The distribution of the phase itself was also derived from chiral perturbation theory. Its simple Gaussian form is consistent with recent lattice simulations [52].

The critical isospin chemical potential beyond which pions Bose-Einstein condense is expected to depend on the temperature. The effect of this shift on the strength of the sign problem is not included in the present paper. In lattice simulations such an effect has been observed [54], and it would of great interest to extend the present work in this direction.

[1] I. M. Barbour, S. E. Morrison, E. G. Klepfish, J. B. Kogut, and M. P. Lombardo, Nucl. Phys. B, Proc. Suppl. **60A**, 220 (1998).

[2] F. Karsch and H. W. Wyld, Phys. Rev. Lett. **55**, 2242 (1985).

[3] J. Flower, S. W. Otto, and S. Callahan, Phys. Rev. D **34**, 598 (1986).

[4] J. Ambjorn, M. Flensburg, and C. Peterson, Nucl. Phys. **B275**, 375 (1986).

[5] Z. Fodor and S. D. Katz, J. High Energy Phys. 03 (2002) 014.

[6] Z. Fodor and S. D. Katz, J. High Energy Phys. 04 (2004) 050.

[7] P. de Forcrand and O. Philipsen, Nucl. Phys. **B642**, 290 (2002).

[8] P. de Forcrand and O. Philipsen, Nucl. Phys. **B673**, 170 (2003).

[9] M. D'Elia and M. P. Lombardo, Phys. Rev. D **67**, 014505 (2003).

[10] R. V. Gavai and S. Gupta, Phys. Rev. D **68**, 034506 (2003).

[11] C. R. Allton *et al.*, Phys. Rev. D **66**, 074507 (2002).

[12] C. R. Allton, S. Ejiri, S. J. Hands, O. Kaczmarek, F. Karsch, E. Laermann, and C. Schmidt, Phys. Rev. D **68**, 014507 (2003).

[13] C. R. Allton *et al.*, Phys. Rev. D **71**, 054508 (2005).

[14] J. Ambjorn, K. N. Anagnostopoulos, J. Nishimura, and J. J. M. Verbaarschot, J. High Energy Phys. 10 (2002) 062.

[15] A. Alexandru, M. Faber, I. Horvath, and K. F. Liu, Phys. Rev. D **72**, 114513 (2005).

[16] Z. Fodor, S. D. Katz, and C. Schmidt, J. High Energy Phys. 03 (2007) 121.

[17] M. Stephanov, Phys. Rev. Lett. **76**, 4472 (1996).

[18] K. Splittorff and J. J. M. Verbaarschot, Nucl. Phys. **B683**, 467 (2004).

[19] J. C. Osborn, Phys. Rev. Lett. **93**, 222001 (2004).

[20] G. Akemann, J. C. Osborn, K. Splittorff, and J. J. M. Verbaarschot, Nucl. Phys. **B712**, 287 (2005).

[21] T. Banks and A. Casher, Nucl. Phys. **B169**, 103 (1980).

[22] J. C. Osborn, K. Splittorff, and J. J. M. Verbaarschot, Phys. Rev. Lett. **94**, 202001 (2005).

[23] E. V. Shuryak and J. J. M. Verbaarschot, Nucl. Phys. **A560**, 306 (1993).

[24] J. J. M. Verbaarschot, Phys. Rev. Lett. **72**, 2531 (1994).

[25] M. L. Mehta, *Random Matrices* (Academic Press, New York, 1967).

[26] Y. V. Fyodorov, B. Khoruzhenko, and H. J. Sommers, Ann. Inst. Henri Poincare Phys. Theor. **68**, 449 (1998).

[27] G. Akemann, Phys. Rev. Lett. **89**, 072002 (2002); J. Phys. A **36**, 3363 (2003).

[28] M. C. Bergere, arXiv:hep-th/0311227; arXiv:hep-th/0404126.

[29] S. F. Edwards and P. W. Anderson, J. Phys. F **5**, 965 (1975).

[30] K. B. Efetov, Adv. Phys. **32**, 53 (1983).

[31] K. Splittorff and J. J. M. Verbaarschot, Phys. Rev. Lett. **98**, 031601 (2007).

[32] K. Splittorff and J. J. M. Verbaarschot, Phys. Rev. D **75**, 116003 (2007).

[33] M. Alford, A. Kapustin, and F. Wilczek, Phys. Rev. D **59**, 054502 (1999).

[34] P. Hasenfratz and H. Leutwyler, Nucl. Phys. **B343**, 241 (1990).

[35] K. Splittorff, D. Toublan, and J. J. M. Verbaarschot, Nucl. Phys. **B620**, 290 (2002); Nucl. Phys. **B639**, 524 (2002).

[36] K. Splittorff and B. Svetitsky, Phys. Rev. D **75**, 114504 (2007).

[37] L. Ravagli and J. J. M. Verbaarschot, Phys. Rev. D **75**, 114504 (2007).

[38] P. E. Gibbs, Report No. PRINT-86-0389 (Glasgow); Phys. Lett. B **182**, 369 (1986).

[39] D. Toussaint, Nucl. Phys. B, Proc. Suppl. **17**, 248 (1990).

[40] T. Schafer, Phys. Rev. D **57**, 3950 (1998).

[41] P. de Forcrand and V. Laliena, Phys. Rev. D **61**, 034502 (2000).

[42] Y. Sasai, A. Nakamura, and T. Takaishi, Nucl. Phys. B, Proc. Suppl. **129**, 539 (2004).

[43] S. Ejiri, Phys. Rev. D **69**, 094506 (2004).

[44] S. Ejiri, Phys. Rev. D **73**, 054502 (2006).

[45] K. Splittorff and B. Svetitsky, Phys. Rev. D **75**, 114504 (2007).

[46] M. D'Elia, F. Di Renzo, and M. P. Lombardo, Phys. Rev. D **76**, 114509 (2007).

[47] S. Conradi and M. D'Elia, Phys. Rev. D **76**, 074501 (2007).

[48] F. Karsch, E. Laermann, and A. Peikert, Nucl. Phys. **B605**, 579 (2001).

[49] J. P. Blaizot, E. Iancu, and A. Rebhan, Phys. Lett. B **523**, 143 (2001).

[50] A. Vuorinen, Phys. Rev. D **68**, 054017 (2003).

[51] J. Liao and E. V. Shuryak, Phys. Rev. D **73**, 014509 (2006).

[52] S. Ejiri, arXiv:0706.3549.

[53] P. H. Damgaard and K. Splittorff, Phys. Rev. D **62**, 054509 (2000).

[54] K. Splittorff, Proc. Sci., LAT2006 (2006) 023.

[55] In the p expansion, the microscopic variables $\mu^2 F_\pi^2 V$ and $m\Sigma V$ are large, and consequently the leading term in the expansion matches the asymptotic limit of the microscopic expression provided that $m_\pi L \ll 1$.